Journal of Mechanical Engineering Research and Developments
ISSN: 1024-1752
CODEN: JERDFO
Vol. 43, No. 5, pp. 89-102
Published Year 2020

A simulation research of heat transfers and chemical reactions in the fuel steam reformer using exhaust gas energy from motorcycle engine

Minh Quang Chau[†], Van Vang Le[‡], Anh Tuan Hoang[††*], Abdel Rahman M. S Al-Tawaha[‡‡], Van Viet Pham[‡*]

[†]Industrial University of Ho Chi Minh City, Ho Chi Minh city, Vietnam

[‡]Ho Chi Minh City University of Transport, Ho Chi Minh city, Vietnam

[††]Ho Chi Minh City University of Technology (HUTECH), Ho Chi Minh city, Vietnam

[‡‡]Al-Hussein bin Talal University, Ma'an, Jordan

*Corresponding Author Email: hatuan@hutech.edu.vn; phamvietmtt@gmail.com

ABSTRACT: Onboard fuel steam reformer heated by the exhaust gas of an internal combustion engine has been considered as an effective device to produce hydrogen (H_2) for engine application. However, the fuel conversion efficiency of the reformer is strongly dependent on heat transfer characteristics between exhaust gas and the reformer. Heat loss of the gas flow along the exhaust system to ambient and the complicated heat and mass transfer inside the reformer with endothermic reforming reactions strongly affect the reformer's efficiency. Therefore, modelling study of heat transfer and chemical reactions is thus necessary, as it is a powerful and cost-effective tool for estimating and maximizing the conversion efficiency and hydrogen yield of the reformer. This paper presents the result of numerical study of heat transfer and chemical reactions in the gasoline steam reformer integrated in engine exhaust system. An onboard compact gasoline steam reformer is made and installed in the exhaust pipe of a Honda Wave motorcycle engine to produce hydrogen continuously by using the waste heat of the engine for heating the reformer. The study accounts for all the aspects of major chemical reactions and heat and mass transfer phenomena in the reformer. A computer simulation code has been developed for the study. The predicted result was validated with experiment data. The results show that by taking advantage of engine exhaust energy, the optimum operating conditions of the reformer under engine full load for high hydrogen yield are at mass water/fuel ratio of 3.5:1 under space velocity of 1000/h. Under these conditions, gasoline conversion of up to 80% and H_2 wet concentration of up to 46% are achieved.

KEYWORDS: waste heat recovery, heat transfer, chemical reactions, fuel stream reformer, SI engine

INTRODUCTION

The emission control of IC engines is always of interest due to more and more stringent emissions standards applied worldwide. Many new engine emission control approaches such as using alternative fuel [1][2], adding hydrogen (H_2) [3] have been studying, in which adding a small proportion of H_2 into the intake charge is an accredited approach for engine effective exhaust emission reduction [4]. However, the storage, distribution and delivery of hydrogen to vehicle engines meet many difficulties because hydrogen is a very light. As a result, the hydrogen-rich gas production by on-board liquid fuel reforming is of interest to overcome the problems [5]. In general, on-board H_2 production can be carried out by reforming of alcohol or hydrocarbons in some ways such as steam reforming (SR), partial oxidation (PO) and auto-thermal reforming (ATR) [6]. SR is probably the most common method for producing H_2. In this process, steam reacts with fuel in the catalyst environment and produce H_2, carbon dioxide and carbon monoxide [7]. This process can yield H_2 concentration up to 70% on dry basic, much higher than PO and ATR [8], but it is strongly endothermic. Therefore, the reformer needs external heat to perform fuel reforming. For the on-board fuel reformer, this required heat can be taken from engine exhaust gas.

There have been many studies on on-board fuel reforming to generate H_2 rich gas for vehicles. Ashur et al [9] studied on-board exhaust gas – gasoline fuel reforming by introducing a certain amount of exhaust gas and gasoline into a reformer heated by the exhaust gas flow in the engine exhaust system. In this case, the reforming process utilizes water vapor and enthalpy from the hot engine exhaust gas to reform the fuel [10]. The study showed that the control of the reformer system is simple but the hydrogen concentration in reformate gas is low, reaching only about 11% by volume. Aydin et al. [11] studied on-board exhaust gas diesel fuel reforming also indicated similar results with hydrogen concentration reaching about 20%. In

general, exhaust gas fuel reforming produces low hydrogen concentration because the water vapor available in the exhaust gas is limited [12]. To improve this situation, in other study, Tsolakis and Megaritis [13] added some water into the reformer and the results showed that hydrogen concentration increased by 15% compared with the case of exhaust gas fuel reforming.

In case of on-board fuel SR for engine application, the use of exhaust gas energy for reformer heating can generate H_2 with an extremely high process efficiency [14]. In fact, the exhaust gas energy normally represents 15%-25% of the total heat energy released from engine fuel combustion [15], which is high enough to heat up the SR reformer and maintains the SR reaction process [16].

Looking back the theoretical basic. It can be said that fuel steam reformer with taking advantage of engine exhaust energy is very appropriate for engine application; therefore, it needs to be deeply studied. To reduce the costs spent on experiments and optimisation of the reformer design for improved its efficiency, modelling study of the SR reformer integrated in engine exhaust system is very important. So far, there have been some modelling studies on predicting the thermal response of the exhaust gas in the exhaust system to improve exhaust pipe design for exhaust energy preservation [17], but very rare detailed modelling work about heat transfer in on-board fuel reformer heated by exhaust gas [18].

The objective of this study is to theoretically investigate the characteristics of heat transfer and catalytic chemical reactions, which affect conversion behavior of on-board gasoline steam reforming to determine optimum operating conditions of the reformer for high hydrogen yield. Because gasoline is a mixture of many hydrocarbons while it has similar properties compared with isooctane C_8H_{18}, isooctane can be used in place of gasoline for mathematical models to simplify the study. The models describe the thermal behavior of engine exhaust gas flowing from the exhaust port along the exhaust pipe and passing the reformer and the response heat and mass transfer and conversion behavior of the reformer. To meet the study objective, the mathematical models for the exhaust pipe and for the reformer are developed and experiment is carried out for the input data determination and model validation.

EXPERIMENTAL SETUP

Figure 1 shows the schematic layout of experimental set-up, in which the test engine is mounted on a hydraulic engine testbed named Didacta T101D. It is a Honda Wave Alpha motorcycle engine, whose specifications are shown in Table 1. The testbed is used for changing engine load. It is also equipped with devices for measuring engine fuel and air consumption to determine the exhaust flow rate. The schematic diagram of the reformer is shown in Figure 2. It is of cylindrical shape, 32 mm in diameter and 100 mm in length, filled with spherical Ni catalyst in length of 80mm (65cm^3) and spherical Al_2O_3 in length of 20mm. The catalyst specifications are shown in Table 1. Reformate gas components were measured using gas analyzers. The concentration of CO and CO_2 were measured using non-dispersive infrared (NDIR) analyzers. The concentration of HC was measured using a heated flame ionization detector (H-FID). NOx was measured using a wet chemiluminescence (CLD) analyzer. Oxygen was measured using oxygen analyzer equipped with an oxygen sensor. Condensed water in steam condensate unit was periodically measured. Hydrogen is calculated from the gas balance analysis.

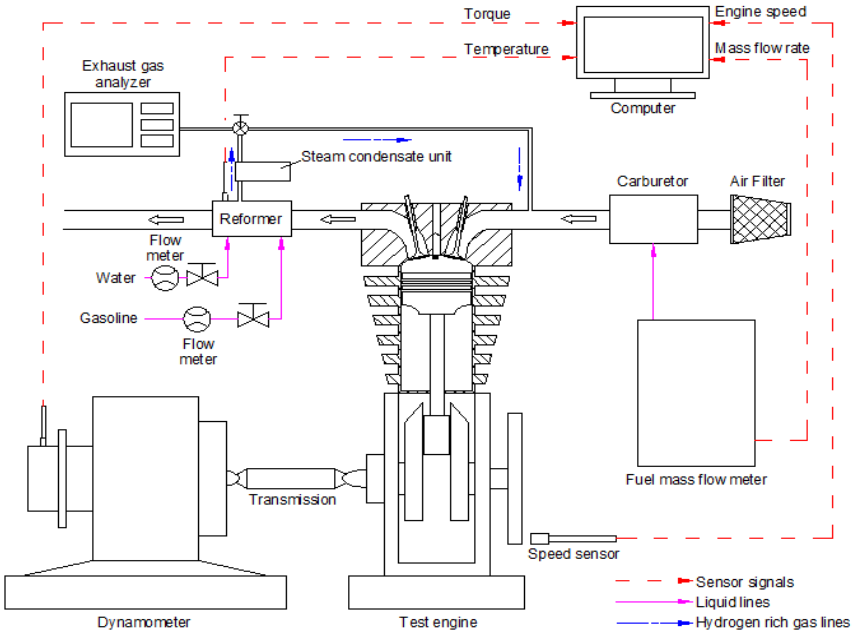

Figure 1. Schematic of experimental set-up

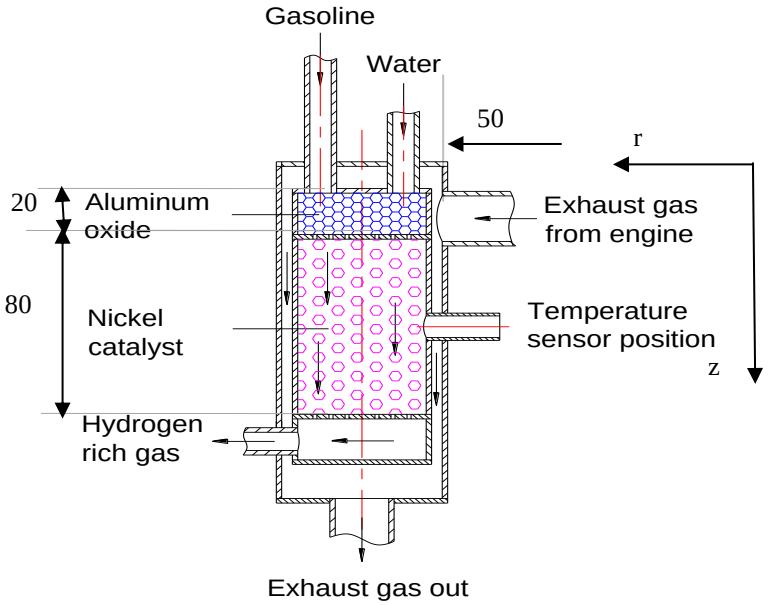

Figure 2. Schematic diagram of on-board steam reformer

Table 1. Engine specifications

Parameters	**Specifications**
Type of engine	Spark ignition, 4 strokes
Number of cylinders	1
Swept volume	97 cm^3
Bore	50 mm
Stroke	49.5 mm
Compression ratio	9.0: 1
Power output	6.5 kW
Revolution	7500 rpm

Table 2. Catalyst properties

Nickel content, wt%	9.8
Alumina content, wt%	balance
Surface area, m^2/g	155
Total pore volume, ml/g	0.9
Size of the sphere, mm	1.75
Average crush strength, N	25

The aim of the experiment is to determine the parameters of engine-out exhaust gas at the exhaust port (temperature, flow rate) at different engine load conditions for input data of the modeling study and to determine the parameters of reformate gas for validation of the theoretical model.

MODELING OF HEAT TRANSFER IN THE EXHAUST PIPE

Governing equations

The heat transfer model simulates thermal response of the exhaust gas and predicts gas temperature along the exhaust pipe. It helps to predict accurate temperature of the exhaust gas heating the fuel reformer.

By assuming quasi-steady, incompressible flow, the energy balance equation for the exhaust gas is written as [19]:

$$\frac{\partial T_g}{\partial t} + u\frac{\partial T_g}{\partial x} = -\frac{q_{gp}}{\rho_g c_{p\,g} V_1} \quad (1)$$

For the exhaust pipe, due to its thin wall associated with high thermal diffusivity of metal, the radial temperature gradient in the pipe wall can be neglected. The energy balance for the pipe wall is then written as:

$$\frac{\partial T_p}{\partial t} = \alpha\frac{\partial^2 T_p}{\partial x^2} + \frac{q_{gp} - q_{cva} - q_{rad}}{\rho_p c_p V_2} \quad (2)$$

Heat transfer from gas to pipe

The heat transfers from exhaust gas to the inner wall:

$$q_{gp} = h_{gp}\pi d_1 \Delta x(T_g - T_{ip}) \quad (3)$$

Heat transfer coefficient h_{gp} is determined by [20]; For a straight pipe:

$$\mathrm{Nu} = \frac{(f/8)(\mathrm{Re})\,\mathrm{Pr}}{1.07 + 12.7(f/8)^{1/2}(\mathrm{Pr}^{2/3} - 1)} \text{ for } 10^4 < \mathrm{Re} < 5\times10^6 \quad \mathrm{Nu} = \frac{(f/8)(\mathrm{Re} - 1000)\,\mathrm{Pr}}{1.07 + 12.7(f/8)^{1/2}(\mathrm{Pr}^{2/3} - 1)} \text{ for } \mathrm{Re} < 10^4 \quad (4)$$

Friction factor (f) was determined by equation (5):

$$\frac{1}{\sqrt{f}} + 2\log\left(\frac{\varepsilon}{3.7d} + \frac{2.51}{\mathrm{Re}\sqrt{f}}\right) = 0 \quad (5)$$

The surface roughness (ε) is 2.59×10^{-4} for cast aluminium tube.

For bend pipe, the effect of pipe bend is accounted for by the following equation [21]:

$$F_B = \frac{\mathrm{Nu}_{bent-pipe}}{\mathrm{Nu}} = 1 + \frac{21 d_1}{\mathrm{Re}^{0.14} d_{bent}} \quad (6)$$

Hence, the Nusselt correlation in equations (4) should be multiplied by F_B to account for the mentioned effects.

Heat conduction from inner surface to outer surface of the exhaust pipe

$$q_{io} = \frac{2\pi k}{\ln(d_2/d_1)}\left(T_{ip} - T_{op}\right) \quad (7)$$

Heat transfer to ambient air

The heat transfer flux from the outer pipe surface to the ambient (q_{cva}) by free convection is:

$$q_{cva} = h_{cva}\pi d_2 \Delta x(T_{op} - T_a);\ h_{cva} = \frac{\mathrm{Nu}\,k_a}{d_2} \quad (8)$$

The Nusselt number can be determined from the following equation [22].

$$\mathrm{Nu} = \left(0.6 + \frac{0.387\mathrm{Ra}^{1/6}}{\left[1 + (0.559/\mathrm{Pr})^{9/16}\right]^{8/27}}\right)^2 \quad (9)$$

$$\mathrm{Ra} = \frac{d_2^3 g\beta(T_{op} - T_a)}{\alpha\nu_a} \quad (10)$$

where property ν is evaluated at temperature $(T_p+T_a)/2$, and property β at T_a. The radiation heat transfer rate from the outer pipe surface to surroundings is expressed as:

$$q_{rad} = \varepsilon \sigma \pi d_2 (T_{op}^4 - T_a^4) \Delta x \quad (11)$$

The set of 2 governing equations (1) and (2) with initial and boundary conditions equations (3) to (11) is then coded in FORTRAN using a finite difference method to solve for the gas temperature along the exhaust pipe from the engine exhaust port to the reformer.

MODELING OF HEAT TRANSFER AND CHEMICAL REACTIONS IN THE REFORMER

Chemical reaction scheme and kinetic mechanisms

The overall reactions in gasoline steam reforming process to form C, CO, CO_2 and H_2O may include the following equations [23].

$C_8H_{18}+8H_2O=8CO+17H_2$; $\Delta H_{1(298)}$ =1310 kJ/mol (12)

$CO+H_2O=CO_2 + H_2$; $\Delta H_{2(298)} = -41$kJ/mol (13)

$C_8H_{18}+16H_2O=8CO_2+25H_2$; $\Delta H_{3(298)}$ =933kJ/mol (14)

Kinetic mechanisms in gasoline steam reforming are very complicated. The detailed analysis of possible mechanisms is presented elsewhere [23][24]. The most appropriate forms of reaction rate expressions for reaction (12), (13) and (14) above for hydrocarbon fuel over nickel catalyst was found in the following form.

$$R_1 = \frac{k_2}{p_{H_2}^{2.5}} \left(p_{C_8H_{18}} p_{H_2O} - \frac{p_{H_2}^3 p_{CO}}{K_{e1}} \right) \times \frac{1}{Q_r^2} \quad (15)$$

$$R_2 = \frac{k_3}{p_{H_2}} \left(p_{CO} p_{H_2O} - \frac{p_{H_2} p_{CO_2}}{K_{e2}} \right) \times \frac{1}{Q_r^2} \quad (16)$$

$$R_3 = \frac{k_4}{p_{H_2}^{3.5}} \left(p_{C_8H_{18}} p_{H_2O}^2 - \frac{p_{H_2}^4 p_{CO_2}}{K_{e3}} \right) \times \frac{1}{Q_r^2} \quad (17)$$

$$Q_r = 1 + K_{CO} p_{CO} + K_{H_2} p_{H_2} + K_{C_8H_{18}} p_{CH_4} + \frac{K_{H_2O} p_{H_2O}}{p_{H_2}}$$

where R_j (kmol/kg cat) is the rate of reaction j (j= 1 – 3); p_{CH_4}, p_{O_2}, *etc.* are, respectively, partial pressures of gas species C_8H_{18}, O_2, *etc.*, $k_j = k_{oj} \times e^{\frac{-E_j}{RT}}$ - the kinetic rate constant of reactions j (j = 1 – 3), in which k_1, k_2, and k_3 are based on Xu and Froment [25]. The kinetic data are shown in Table 3. k_{oj} is constant, E_j (kJ/kmol) - gas constant; T (K) - the gas temperature in the reaction zone; K_{ej} - the equilibrium constant of reaction j (j =1 – 3) and can be found in Table 4; $K_i = K_{oi} \times e^{\frac{-\Delta H_i}{RT}}$ - the adsorption constant of species CO, H_2, C_8H_{18}, H_2O in reactions (12), (13), (14), which can be found in Table 5.

The rate of consumption or formation of an individual gas species based on reactions (12) to (14) is determined by summing up the reaction rates of that species in all three reactions and consider the intraparticle mass transport limitations by multiplying the rates (15) to (17) with various effectiveness factors η_1, η_2, and η_3 [24].

As a result, the conversion rates of the individual species are as follows:

$$r_{C_8H_{18}} = -\eta_1 R_1 - \eta_3 R_3 \quad (18)$$

$$r_{CO_2} = \eta_2 R_2 + 8\eta_3 R_3 \quad (19)$$

$$r_{H_2O} = -8\eta_1 R_1 - \eta_2 R_2 - 16\eta_3 R_3 \quad (20)$$

$$r_{CO} = 8\eta_1 R_1 - \eta_2 R_2 \quad (21)$$

$$r_{H_2} = 17\eta_1 R_1 + \eta_2 R_2 + 25\eta_3 R_3 \quad (22)$$

where r_i is the conversion rate of gas species i (C_8H_{18}, CO_2, *etc*.).

Table 3. Kinetic parameters

Reaction	k_{oj} (kmol/kgcat.h)	E_j (kJ/kmol)
1	4.225×10^{15} bar$^{0.5}$	240100
2	1.955×10^{6} bar^{-1}	67130
3	1.020×10^{15} bar $^{0.5}$	243900

Table 4. Equilibrium constants

Reaction	Equilibrium constant K_{ej}
1	5.75×10^{12} exp(-11476/T) (bar^2)
2	1.26×10^{-2} exp(4639/T)
3	7.24×10^{10} exp(-21646/T) (bar^2)

Table 5. Adsorption constants

Species	K_{oi} (bar $^{-1}$)	ΔH_i (kJ/kmol)
C_8H_{18}	6.65×10^{-4}	-38280
CO	8.23×10^{-5}	-70650
H_2	6.12×10^{-9}	-82900
H_2O	1.77×10^{5} bar	88680

Reformer modeling

Figure 3 shows the schematic diagram of a 2-D steam reformer heated by exhaust gas. The reformer is of cylindrical shape, 32 mm in diameter and 100 mm in length, filled with alumina in 20mm and Ni catalyst in 80mm of reformer length. Catalyst specifications are shown in Table 2. The hot exhaust gas flows around the reformer to heat it to its operation temperature.

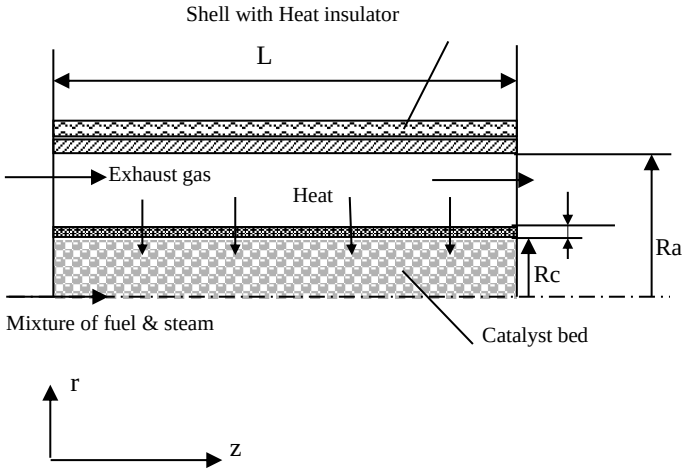

Figure 3. Schematic diagram of a 2-D steam reformer

In on-board steam reforming, since the reformer normally operates at a temperature lesser than 700ºC, the heat radiation can be omitted. To simplify the model, one may assume that the gas properties and flow at the inlet cross-section of the reformer are uniform. The phenomena in the reformer include chemical reactions on the catalyst surface, heat and mass transfers in the axial and radial directions of the reformer in the solid phase and gas phase. The pressure drop is assumed to be negligible. With these assumptions a 2-D reformer model is most appropriate to describe the reforming behavior under the mentioned conditions. However, because in the axial direction, the dispersion coefficient is much smaller than the gas velocity, it can be ignored without significant influence on the calculation results. In addition, the heat conductivity of gas is much smaller than that of catalyst bed, it can be omitted. Moreover, in the gas phase the change of gas properties and concentrations with time is normally much smaller than that with space, especially when the operation approximately reaches to steady state, hence it can be ignored within a small step time.

Governing equations

Heat transfer from exhaust gas to the reformer wall is expressed by the energy balance equations for the control volume of the exhaust gas in the exhaust gas site and for the control volume of reformer wall, which are written as:

$$u_{exh}\frac{\partial T_{exh}}{\partial z} = -\frac{q_{exh-p}}{\rho_{exh}c_{p\,exh}V_{exhz}} \tag{23}$$

$$\frac{\partial T}{\partial t} = \alpha\frac{\partial^2 T}{\partial z^2} + \frac{q_{exh-p} - q_{p=g}}{\rho_p c_p V_{pz}} \tag{24}$$

where u_{exh}, T_{exh} are exhaust gas velocity and temperature in the exhaust site; $q_{exh\text{-}p}$ is heat transfer from exhaust gas to reformer wall; ρ_{exh}, c_{pexh}, V_{exhz} are density, specific heat, control volume of exhaust gas; T, ρ_p, c_p, V_{pz} are temperature, density, specific heat, control volume of the reformer wall; α is heat transfer coefficient from exhaust gas to the reformer wall surface; $q_{p\text{-}g}$ is heat transfer from reformer wall to the gas in the reformer.

In the reformer, with the assumptions mentioned above, the basic equations of the model based on the mass and energy balance for the gas phase and solid phase of the reformer are written as follows.

$$u\frac{\partial C_i}{\partial z} = D_{dpi}\left(\frac{\partial^2 C_i}{\partial r^2} + \frac{1}{r}\frac{\partial C_i}{\partial r}\right) + \rho_{cat}r_i \tag{25}$$

$$\varepsilon\rho_g c_{pg}\frac{\partial T_g}{\partial t} = -u\rho_g c_{pg}\frac{\partial T_g}{\partial z} + S_h h(T - T_g) \tag{26}$$

$$\rho_b c_{pb}\frac{\partial T}{\partial t} = K\left(\frac{\partial^2 T}{\partial r^2} + \frac{1}{r}\frac{\partial T}{\partial r} + \frac{\partial^2 T}{\partial z^2}\right)$$

$$+S_h h(T_g - T) + \rho_{cat}\sum_{j=1}^{4}(-\Delta H_j)R_j \tag{27}$$

where i denotes the gas species; j - reaction index; ρ_g, ρ_{cat}, ρ_b (kg/m^3) - the densities of gas, catalyst and bulk catalyst bed, respectively; c_{pg} and c_{pb} (J/kgK) - the specific heats of gas and of catalyst bed, respectively; ε - the void fraction of the catalyst bed; h_{Di} (m/s) - the mass transfer coefficient of gas component i; h (W/m^{2}K) - the heat transfer coefficient; T and T_g (K) - the temperature of solid phase and gas phase, respectively; C_i (mol/m^3) - the concentration of gas species i; r and z (m) - cylindrical coordinates; S_h (m^2/m^3) - the heat transfer area per volume of catalyst bed; ΔH_j (J/mol) - the heat of reaction j; K (W/mK) - the heat conduction coefficient of catalyst bed; D_{dpi} - the dispersion coefficient of gas component i; u (m/s) - the superficial gas velocity equal to the ratio of volume flow rate to the cross section area of the reformer.

The dispersion coefficient of gas in a catalyst bed is dependent on molecular gas diffusion, bulk gas velocity and pellet diameter and can be determined based on Askcan et al. [26] as: $D_{dpi} = \varepsilon\left(\frac{D_i}{\tau_{bed}} + 0.5 d_p u\right)$; where d_p is pellet diameter; D_i is gas diffusivity of species i to the mixture of the other gas in the reactor; τ_{bed} is tortuosity of the bed and correlated to the

void fraction of catalyst bed ε as: $\tau_{bed} = \frac{1}{\sqrt{\varepsilon}}$.

Based on the phenomena of the gas flow and operating conditions of the reformer, the initial and boundary conditions are set as follows:

$$\text{At } t = 0: T = T_o; \tag{28}$$

At reformer inlet face $z = 0$:

$$T_{exh} = T_{exh}^{in},\ T_g = T_g^{in};\ C_i = C_i^{in} \tag{29}$$

$$\text{At reformer outlet face } z = L: \ \frac{\partial C_i}{\partial z} = 0;\ \frac{\partial T_g}{\partial z} = 0; \tag{30}$$

$$\text{At the centre } r = 0: \quad \frac{\partial C_i}{\partial r} = 0; \quad \frac{\partial T_g}{\partial r} = 0; \tag{31}$$

$$\text{At the interfacial surface of inner reformer wall and catalyst bed } r = R: \ \frac{\partial C_i}{\partial r} = 0; \tag{32}$$

where T_h is the temperature of reformer wall; α - the overall heat transfer coefficient through the reformer wall; K (W/mK) - the heat conduction coefficient of the catalyst bed and gas, respectively. The properties of gas, ρ_g & c_{pg}, depend on temperature and composition of the gas mixture. k_g depends on temperature and heat capacity of gas and, hence, also depends on the composition of the gas mixture. Therefore, these properties vary from one location to the other in the reformer and vary with time. They are determined from the properties and mass fractions of the individual species of the gas mixture, whose properties can be taken from [27] as algebraic functions of temperature. Therefore, at each point in the reformer volume, once the temperature and mole or mass fractions of the gas mixture are known, the overall properties can be determined.

Heat and mass transfer coefficients

The heat transfer coefficient between catalyst and gas, h ($W/m^2 \cdot K$), is determined using Colburn factor J_H [28]:

$$h = J_H \frac{c_{pg} G_o}{(Pr)^{2/3}} \tag{33}$$

$$J_H = 0.91 Re^{-0.51} \psi, \ (Re<50)$$

$$J_H = 0.61 Re^{-0.41} \psi, \ (Re>50)$$

$$Re = \frac{G_o}{S_{geo} \mu_g \psi}$$

where Pr is the Prandtl number of the gas flow in the reformer; G_o ($kg/(s \cdot m^2)$) is the superficial mass flow rate, which is defined as mass flow rate $\dot{m}$ divided by the cross section area S of the reformer.

The overall heat transfer coefficient through the reformer wall, K, is determined from:

$$\frac{1}{K} = \frac{1}{h_i} + \frac{b}{\lambda} \tag{34}$$

where $\frac{b}{\lambda}$ is thickness of the reformer wall (m); h_i is the heat transfer coefficient on the inside of the reformer wall (W/m^{2}K), while is the heat conduction coefficient of the reformer wall (W/mK), which can be taken from [29]; h_i is given by Cengel et al. [30].

The reformer is studied onboard of a motorcycle engine with swept volume of 110 cm^3, brake power of 6.5 kW/7500 rpm. In this case, exhaust gas flowing around the reformer is at flow-rate of 25 kg/h and temperature above 650^{o}C. The set of 5 governing equations (23) to (27) with initial and boundary conditions equations (28) to (32), combined with the heat and mass transfer coefficients, equations (33, 34), is then coded in FORTRAN using a finite difference method to solve for the temperature and gas concentration along and across the reformer. The overall temperature and compositions of the products are derived from the predicted values at different space elements at the rear face of the reformer, based on the principle of mixing gas.

SIMULATION RESULT AND DISCUSSIONS

Table 6. Exhaust gas parameters at exhaust port

Engine load level	100%	75%	50%
Mass flow rate (g/s)	5,6	4,9	3.5
Temperature (degree C)	712	695	650

The exhaust gas parameters at engine exhaust port used as input data for the models are measured under different load level at the engine speed of 7500 rpm. The typical measured data are shown in Table 3. Fuel supplied to the reformer is fixed at flow rate of 110 g/h, equal to 5% of fuel consumption of the engine at full load. Water to fuel ratio in mass (W/F) varies from 1 to 5. Hence, at the highest gas flow rate, the corresponding space velocity (SV) of the gas is about 1000/h, much less than the normal limit value of 15000/h required for SV of a fuel reforming. The typical modeling results are plotted and shown in Figures 4 to 10.

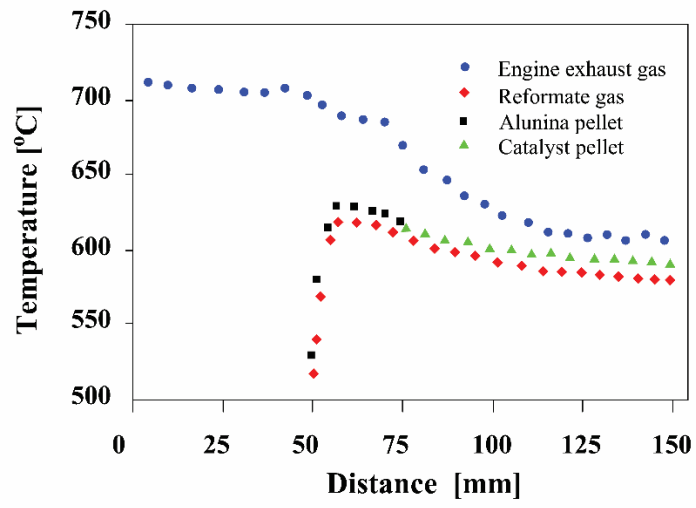

Figure 4. Temperatures of exhaust gas, alumina pellet, catalyst pellet and gas in the reformer along the exhaust pipe and reformer, W/F=3.5, under engine full load

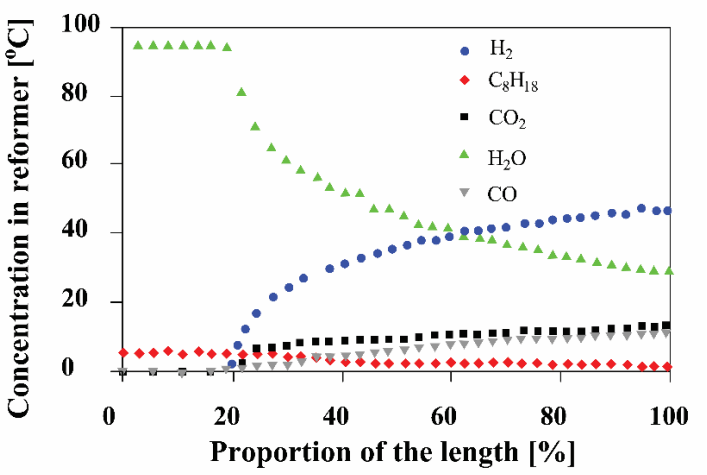

Figure 5. Gas conversion in the reformer along its length with W/F=3.5 under engine full load

Figure 4 describes the variation of engine exhaust temperature, alumina pellet mean temperature, catalyst mean temperature and mean temperature of gas in the reformer along the exhaust pipe and reformer under engine full load and W/F=3.5. The exhaust temperature decreases continually but at different rates corresponding to different pipe sections. In the first section (50mm), the gas temperature decreases not much because this section is short, and the heat loss is only due to free convection at the outer surface of the pipe. In the second section, the exhaust gas temperature decreases faster than that in the first because heat loss here is not only due to free convection but also warming up and vaporizing fuel and water. In the third section, the exhaust gas temperature decreases significantly due to heat loss to the endothermic steam reforming reactions in the reformer and free convection at the outer surface. Alumina pellet are placed in the front part of the reformer (20mm). They are heated by exhaust gas but cooled by water and fuel supplied to the reformer. As a result, the alumina pellets closer to the entry of fuel and water has lower temperature. Catalyst pellets are placed after the alumina pellets in the reformer (80mm) and heated by exhaust gas but cooled by very endothermic reforming reactions. As a result, the catalyst temperature decreases continually along the reformer.

The gas in the reformer is directly heated by the catalyst pellet, hence its temperature is a little lower than that of catalyst, but the profiles are similar. Figure 5 shows the variation of species concentration of reformate gas along the reformer. It indicates that in the alumina zone, there exist only fuel and water vapors. In the catalyst zone along the reformer, fuel and water decrease while CO, CO_2 and H_2 increase. This means that the reforming reactions take place, consuming fuel and water, producing CO, CO_2 and H_2. At engine full load and W/F=3.5, fuel conversion reaches 80%, H_2 concentration reaches 46%, CO- 11%, CO_2- 10%, H_2O down to 29% at the exit of the reformer.

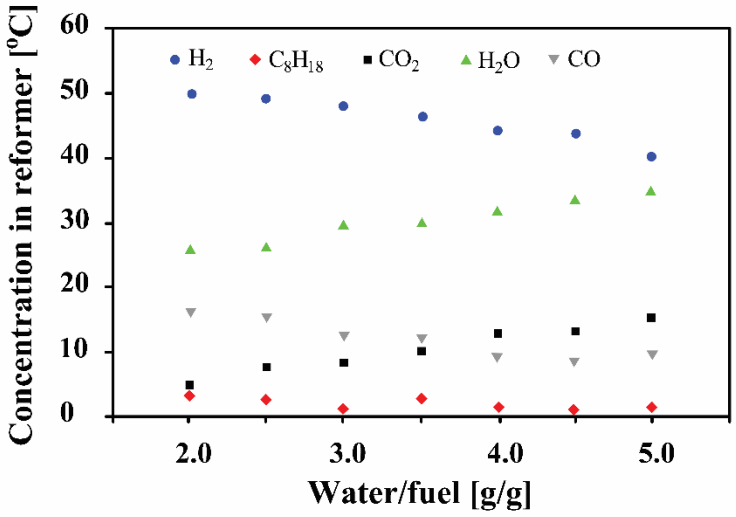

Figure 6. Reformate gas concentration at the outlet of the reformer at different W/F under engine full load

Figure 6 shows concentrations of reformate gas at the outlet of the reformer at different W/F under engine full load. As can be seen from the figure, increasing W/F leads to the increase in CO_2 concentration. This means that more water gas-shift reactions take place. Consequently, more H_2 is produced; however, the figure indicates the decrease of H_2 wet concentration. This may be due to the increased H_2O concentration present in the reformate gas.

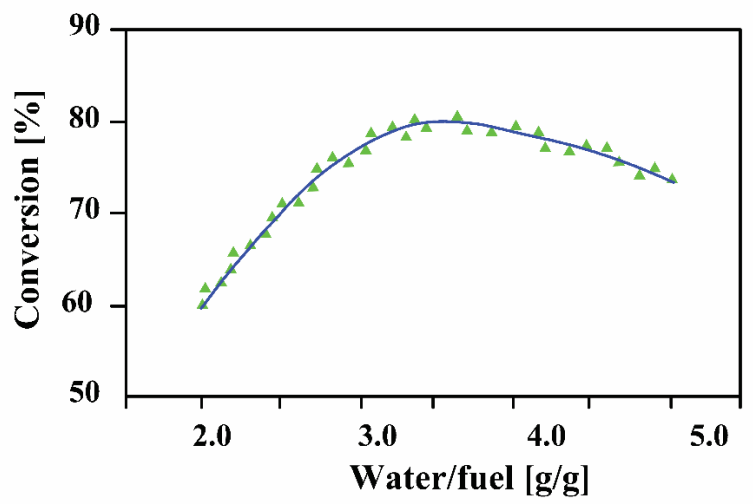

Figure 7. Gasoline fuel conversion at different mas W/F under engine full load

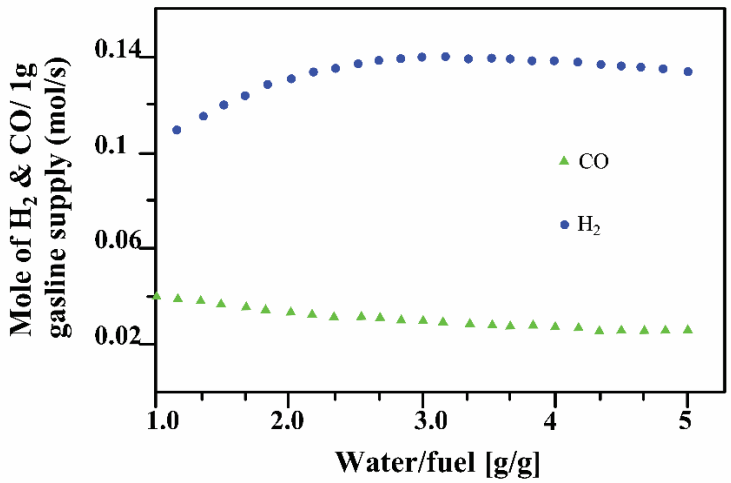

Figure 8. Mole of H_2 and CO produced per 1 gram of fuel at different mass W/F under engine full load

The effect of W/F on fuel conversion efficiency and H_2 and CO generation can be seen clearer in Figure 7 and Figure 8, which show fuel conversion efficiency and the number of moles of H_2 and CO produced per 1 gram of fuel at different mass W/F under engine full load. With W/F=3.5, the highest amount (0.14 mol) of H_2 is produced from 1 gram of fuel and fuel conversion efficiency reaches to highest value of 80%. Low W/F causes the lack of water for steam reforming and water gas-shift reactions. This causes low fuel conversion efficiency and high CO and low H_2 generations. High W/F will demand more heat for vaporizing water and the remaining of heat for fuel reforming decreases, leading to the decrease in fuel reforming reaction and therefore the decrease in fuel conversion efficiency.

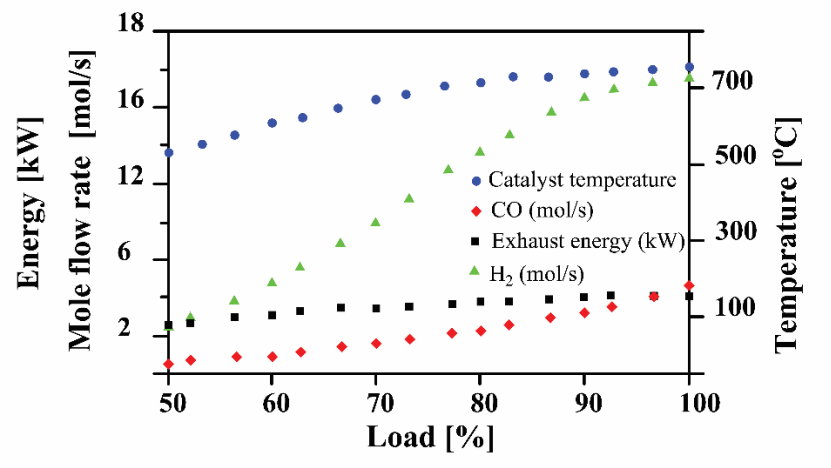

Figure 9. Engine exhaust gas energy, catalyst mean temperature and mole flow rate of H_2 and CO produced by the reformer at different engine load level

Figure 9 indicates the engine exhaust gas energy, catalyst mean temperature and mole flow rate of H_2 and CO produced by the reformer at different engine load level. As can be seen from the figure that increasing engine load causes the increase of exhaust gas energy because of the increase in both temperature and flow rate of exhaust gas. This increases catalyst heating and hence raising the catalyst temperature, which help to increase fuel conversion efficiency and generate more H_2 and CO.

Validation of the mathematical model

Figure 10 compares the predicted and measured reformate gas component concentration at mass W/F=3.5, fuel flow rate of 110 g/h to reformer, under engine full load. The effectiveness factors of kinetic data have been appropriately chosen to assure that the difference between the predicted and measured data is less 5%.

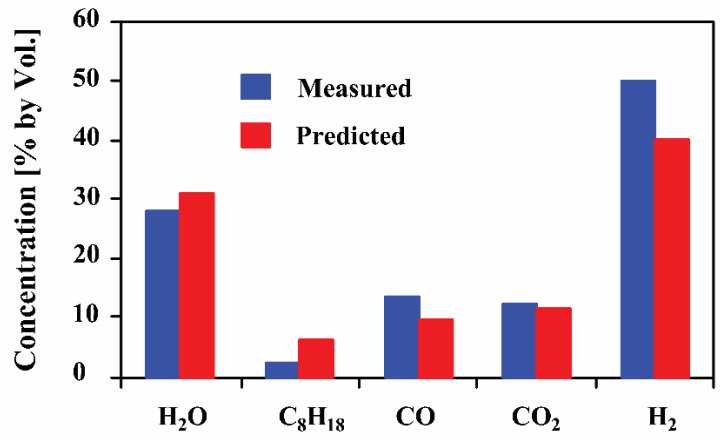

Figure 10. Comparison of predicted and measured reformate gas component concentration at mass ratio W/F=3.5, fuel flow rate of 110 g/h to reformer, under engine full load

CONCLUSION

The 2-D on-board gasoline steam reformer model accounted for all the aspects of heat transfer and chemical reactions has been developed. The simulation program allows to determine any gas parameters at any space position of the exhaust pipe and the reformer and at any time from the start of reforming operation. The optimum conditions for high fuel conversion and high hydrogen yield at engine full load are with W/F of 3.5:1 in mass basis under space velocity of about 1000/h. Under these conditions, gasoline conversion of up to 80% and H_2 wet concentration of up to 46% are achieved and 1 gram of gasoline can produce 0.14 moles of hydrogen. The on-board reformer can be heated enough by engine exhaust gas energy to reform the

fuel flow rate of 110g/h, representing 5% of the fuel that the engine consumed. The study confirms that on-board gasoline steam reforming taking advantage of engine exhaust gas energy is a convenient and effective method to produce hydrogen-rich gas for engine application.

REFERENCES

[1] A. T. Hoang, "Waste heat recovery from diesel engines based on Organic Rankine Cycle," *Appl. Energy*, vol. 231, pp. 138–166, 2018.

[2] V. V. Pham and A. T. Hoang, "Technological perspective for reducing emissions from marine engines," *Int. J. Adv. Sci. Eng. Inf. Technol.*, vol. 9, no. 6, pp. 1989–2000, 2019.

[3] T. D'Andrea, P. F. Henshaw, and D. S. K. Ting, "The addition of hydrogen to a gasoline-fuelled SI engine," *Int. J. Hydrogen Energy*, 2004.

[4] A. T. Hoang and V. V. Pham, "A study on a solution to reduce emissions by using hydrogen as an alternative fuel for a diesel engine integrated exhaust gas recirculation," in *International Conference On Emerging Applications In Material Science And Technology: ICEAMST 2020*, 2020.

[5] S. C. Chen, Y. L. Kao, G. T. Yeh, and M. H. Rei, "An onboard hydrogen generator for hydrogen enhanced combustion with internal combustion engine," *Int. J. Hydrogen Energy*, 2017.

[6] J. C. Martin, P. Millington, B. Campbell, L. Barron, and S. Fisher, "On-board generation of hydrogen to improve in-cylinder combustion and after-treatment efficiency and emissions performance of a hybrid hydrogen–gasoline engine," *Int. J. Hydrogen Energy*, 2019.

[7] A. T. Hoang *et al.*, "Power generation characteristics of a thermoelectric modules-based power generator assisted by fishbone-shaped fins: Part II–Effects of cooling water parameters," *Energy Sources, Part A Recover. Util. Environ. Eff.*, pp. 1–13, 2019.

[8] A. T. Hoang and M. Q. Chau, "A mini review of using oleophilic skimmers for oil spill recovery," *J. Mech. Eng. Res. Dev.*, vol. 41, no. 1, pp. 92–96, 2018.

[9] M. Ashur *et al.*, "On board Exhaust Gas Reforming of Gasoline Using Integrated Reformer & TWC," in *SAE Technical Papers*, 2007.

[10] B. Yang, G. Song, L. Shen, Y. A. Ghuktomova, and J. Xu, "Fault Diagnosis Method for Internal Combustion Engines Based on IHS-RVM Model," *J. Mech. Eng. Res. Dev.*, vol. 40, no. 1, pp. 64–71, 2017.

[11] K. Aydin and R. Kenanoğlu, "Effects of hydrogenation of fossil fuels with hydrogen and hydroxy gas on performance and emissions of internal combustion engines," *Int. J. Hydrogen Energy*, 2018.

[12] A. T. Hoang, X. L. Bui, and X. D. Pham, "A novel investigation of oil and heavy metal adsorption capacity from as-fabricated adsorbent based on agricultural by-product and porous polymer," *Energy Sources, Part A Recover. Util. Environ. Eff.*, vol. 40, no. 8, pp. 929–939, 2018.

[13] A. Tsolakis and A. Megaritis, "Catalytic exhaust gas fuel reforming for diesel engines - Effects of water addition on hydrogen production and fuel conversion efficiency," *Int. J. Hydrogen Energy*, 2004.

[14] A. T. Hoang and V. V. Pham, "A study of emission characteristic, deposits, and lubrication oil degradation of a diesel engine running on preheated vegetable oil and diesel oil," *Energy Sources, Part A Recover. Util. Environ. Eff.*, vol. 41, no. 5, pp. 611–625, 2019.

[15] A. T. Hoang and V. V. Pham, "Impact of Jatropha Oil on Engine Performance, Emission Characteristics, Deposit Formation, and Lubricating Oil Degradation," *Combust. Sci. Technol.*, 2018.

[16] L. Tartakovsky and M. Sheintuch, "Fuel reforming in internal combustion engines," *Progress in Energy and Combustion Science*. 2018.

[17] V. V. Pham, "An optimal research for diesel engine using biofuels fuel when considering the effects of the change of parameters on ECU," in *AIP Conference Proceedings*, 2020.

[18] A. T. Hoang and A. T. Le, "A review on deposit formation in the injector of diesel engines running on biodiesel," *Energy Sources, Part A Recover. Util. Environ. Eff.*, vol. 41, no. 5, pp. 584–599, 2019.

[19] Y. S. Rudy, Nukman, R. Sipahutar, A. Aipon, P. Rahmadi, and A. T. Arief, "Mechanical properties of castings aluminium waste which is smelted in simple furnace with a variety of fuels," *J. Mech. Eng. Res. Dev.*, vol. 40, no. 4, pp. 692–698, 2017.

[20] D. M. McEligoi, "Fundamentals of momentum, heat and mass transfer," *Int. J. Heat Mass Transf.*, 1970.

[21] S. El Bécaye Maïga, S. J. Palm, C. T. Nguyen, G. Roy, and N. Galanis, "Heat transfer enhancement by using nanofluids in forced convection flows," *Int. J. Heat Fluid Flow*, 2005.

[22] S. W. Churchill and H. H. S. Chu, "Correlating equations for laminar and turbulent free convection from a horizontal cylinder," *Int. J. Heat Mass Transf.*, 1975.

[23] M. Pacheco, J. Sira, and J. Kopasz, "Reaction kinetics and reactor modeling for fuel processing of liquid hydrocarbons to produce hydrogen: Isooctane reforming," *Appl. Catal. A Gen.*, 2003.

[24] A. M. De Groote and G. F. Froment, "Simulation of the catalytic partial oxidation of methane to synthesis gas," *Appl. Catal. A Gen.*, 1996.

[25] J. Xu and G. F. Froment, "Methane steam reforming, methanation and water-gas shift: I. Intrinsic kinetics," *AIChE J.*, 1989.

[26] A. Alimoradi and F. Veysi, "Prediction of heat transfer coefficients of shell and coiled tube heat exchangers using numerical method and experimental validation," *Int. J. Therm. Sci.*, 2016.

[27] "Book Review:Fundamentals of Heat and Mass Transfer," *Chem. Eng. Res. Des.*, 2007.

[28] W. M. Dean, "Analysis of Transport Phenomena," *Oxford Univ. Press*, 2017.

[29] S. D. Holdsworth and R. Simpson, "Heat Transfer," in *Food Engineering Series*, 2016.

[30] Y. Cengel, R. Turner, and R. Smith, "Fundamentals of Thermal-Fluid Sciences," *Appl. Mech. Rev.*, 2001.